A Novel Parallel Flow Control (PFC) System for Syringe-Driven Nanofluidics

H. Liang, Wook Jun Nam and Stephen J. Fonash

Center for Nanotechnology Education and Utilization
The Pennsylvania State University, University Park, PA, USA, hzl114@psu.edu

ABSTRACT

Active nanofluidic flow control is accomplished by utilizing the parallel flow control (PFC) configuration and it allows the primary problems of nanofluidic systems, including interfacing and measuring, to be overcome. PFC uses flow in a syringe-driven micro-channel, which interfaces with the "outside world", to set up the pressure gradient across a nano-channel. Based on the size-scale differences between these nano- and micro-channels arranged in parallel, nano- to micro-channel flow rate ratios of 10^{-4}:1 and smaller are easily attainable thereby allowing the attainment of a broad range of fine nanofluidic flow control. Long residence time and non-uniform flow rate issues are easily avoided by driving a relative large flow rate through the micro-channel. Direct, real-time flow rate measurements in the nano-channel are achieved by having an additional serpentine measurement micro-channel in series with the nano-channel. Nano-channel flow rates as low as ~0.5 pL/s are measured.

Keywords: nanofluidic flow control, nanofluidics, nano-total analysis systems, miniaturized chemical processing

1 INTRODUCTION

The use of nanofluidics for new sensing and chemical reaction approaches has yet to be exploited due to challenges that must be overcome[1]. The basic hindrances to nanofluidics utilization lie in integrating, interfacing, and controlling nanofluidics to realize active flow control and flow characterization. At present, most of the nanofluidic systems are based on a diffusion mode of fluid manipulation [2, 3] which can be impracticable for many situations. Pressure-driven flow using a syringe pump is simpler and has a broad range of applicability for producing transport in nano-scale channels since it simply relies on mechanical pressure. However, previously explored nano-scale pressure-driven approaches have either had excessive sample residence times or system complexity issues[4,5] due to the extremely tiny volumes of nanofluidic systems (on the order of femto-liter).

This work uses a novel active nanofluidic flow control configuration to address the primary problems of nanofluidic systems including interfacing and measuring. We term this approach, which is seen in Fig. 1, parallel flow control (PFC). It uses flow in the syringe-driven micro-channel which is in parallel with nano-channel and which interfaces with the "outside world", to set up the pressure gradient across the nano-channel to control the nanofluidic flow. It also uses a serpentine micro-channel in series with the nano-channel to measure the nanofluidic flow.

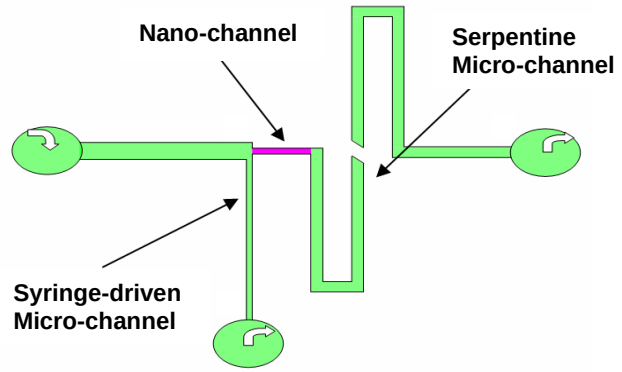

Figure 1. Schematic of the parallel flow control (PFC) approach for nanofluidic flow control. The pressure gradient across the nano-channel is controlled by the syringe-driven micro-channel flow in parallel with nano-channel. The serpentine micro-channel is in series with nano-channel to measure the nanofluidic flow rate by tracking the water-air interface.

2 DEVICE FABRICATION

The devices in this work were fabricated using two-step etching and glass bonding techniques in a class-10/100 cleanroom. The fabrication processes are CMOS compatible allowing potential application in future integrated micro-/nano-total analysis systems. The overall fabrication processes began with dry etching the nano-channel (100nm high, 15 μ m wide, and 200 μ m long) into a glass wafer. Then both syringe-driven micro-channel (10 μ m high, 10 μ m wide, and 4350 μ m long) and serpentine micro-channel (10 μ m high, 20 μ m wide, and 8cm long) were patterned in alignment with the nanofluidic channel using wet chemical etching (6:1 buffered oxide etchant). Finally, after drilling the accessing ports through the glass wafer, it was bonded with another blank glass wafer to finish the fabrication. A completed, actual PFC device is seen in Fig. 2 with DI water infused.

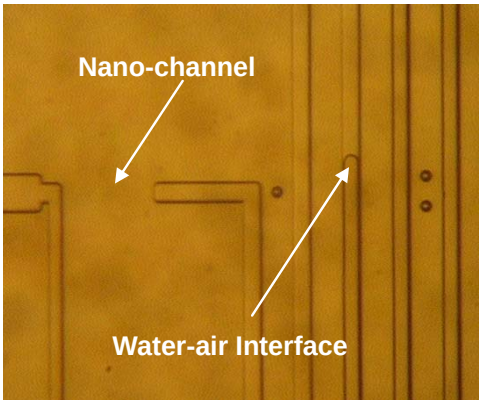

Figure 2. Bonded PFC nanofluidic flow control system with water infused by a syringe pump. The water-air interface is visible in the serpentine micro-channel in series with nano-channel.

3 THEORETICAL ANALYSIS

PFC is able to control the nano-channel flow by using the flow through the syringe-driven micro-channel. Therefore, an assessment of the flow rate ratios between nano- and micro-channel available using PFC can be established by using the simple flow model sketched in Fig. 3.

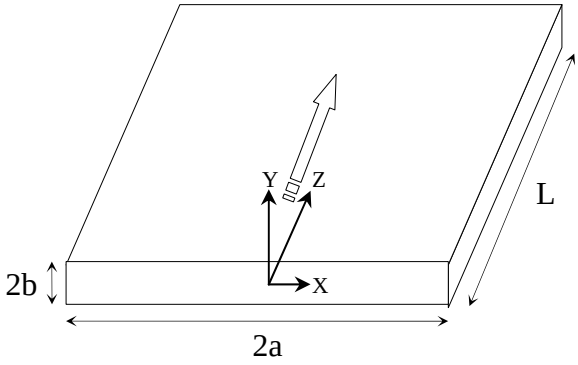

Figure 3. Schematic of fluidic flow model. Here 2a and 2b are channel width and height respectively.

Assuming a single one phase Newtonian fluid in the channel shown and a constant pressure gradient $-dp/dz = \Delta p/L$ along the flow direction, where Δp is the pressure drop along a given channel and L is the channel length, it follows from mass conservation and momentum conservation that the flow rate ratio Q_n/Q_m between nano- and micro-channel can be written as[6]

$$\frac{Q_n}{Q_m} = \frac{b_n^3 \sum_{n=1,3,5,\ldots}^{\infty} \left[a_n - \frac{2b_n}{n\pi} \tanh(n\pi a_n / 2b_n) \right] \frac{L_m}{n^4}}{b_m^3 \sum_{n=1,3,5,\ldots}^{\infty} \left[a_m - \frac{2b_m}{n\pi} \tanh(n\pi a_m / 2b_m) \right] \frac{L_n}{n^4}} \qquad (1)$$

where a and b is the channel width and height respectively.

We can see from Eq. (1) that this flow rate ratio can be used to control a very precise (fine) flow through a nano-channel in parallel to a micro-channel. The flow rate ratio of Q_n/Q_m can be of the order of 10^{-4} or smaller for nano- and micro-channel. This is analogous to controlling the electric current through one large resistor by connecting a smaller resistor in parallel (Fig. 4).

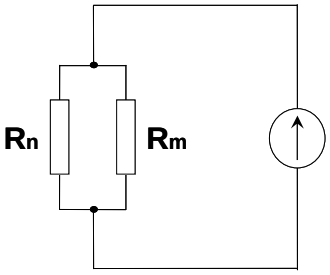

Figure 4. The electric circuit model corresponding to the nanofluidic flow control system. Rn and Rm represent the flow resistance of nano-channel and syringe-driven micro-channel, respectively. The current source represents the flow rate source controlled by a syringe pump. The flow through the nano-channel can be controlled by the flow through the syringe-driven micro-channel with the flow rate ratio decided by Eq. (1).

4 EXPERIMENTAL RESULTS

An assessment of PFC approach was undertaken by comparing the calculated nano-channel flow rate using the flow rate ratio of the nano- and micro-channels (~7.7×10^{-5}:1 from Eq. (1)) with experimental flow rate measurements determined by optically tracking the water-air interface in the serpentine micro-channel (Fig. 2). For this experiment, DI water was infused through the system at different flow rates controlled by a syringe pump. The results are shown in Fig. 5. As can be seen from this figure, either way of assessing the nano-channel flow rate shows extremely fine nanofluidic flow rates and flow control is possible with the PFC approach.

The fact that the experimental nano-channel flow rate is about 22 times slower than the calculated flow rate shown in Fig 5 is due to dimension control during the etching. That is, isotropic wet etching of the syringe-driven micro-channel and of the serpentine micro-channel do not produce the rectilinear cross-section shown in Fig.3 and used in Eq. (1). This wet etching produces an undercut profile and thereby makes the widths of these micro-channels larger than that designed and the channel cross-section far from rectilinear. For example, based on the isotropic etching geometry and etching depth into the glass substrate (10 μ m), the actual serpentine micro-channel cross-section area is estimated to actually be 78.5% larger than what was designed. This larger serpentine micro-channel width dimension resulting from isotropic wet etching means that

NSTI-Nanotech 2008, www.nsti.org, ISBN 978-1-4200-8505-1 Vol. 3

the actual nano-channel flow is larger than that given by the experimental curve of FIG. 5. Using this increased cross-sectional area value leads to the "adjusted experimental values" curve seen in FIG. 5. This processing-caused increase in the syinge-driven micro-channel cross-section has a corresponding impact on the calculated curve of FIG. 5 because Eq (1) is no longer valid since the rectilinear cross-section of Fig 3 does not apply. By using a computational analysis[7] employing the correct cross-section shape and size to replace Eq. (1), we can re-determine the Q_n/Q_m ratio, which is multiplied times the syringe flow rate to get the calculated nano-channel flow rate. For the case of the device of Fig. 2 this re-calculated Q_n/Q_m decreased to 2.37×10^{-5}. Use of this re-calculated ratio results in the "adjusted calculated values" curve also shown in FIG. 5. As seen, the adjusted experimental flow rate is about 4 times slower than the adjusted theoretical value. We believe this difference is due to some combination of wetting effects, interactions with the walls[4], and evaporation effects in the serpentine micro-channel[8]. As seen from Fig. 5, the smallest nano-channel flow rate is ~0.5 pL/s. While not the lower limit of the PFC flow rates achievable, this value already compares well with the previously reported, smallest flow rate of 30 pL/s[8].

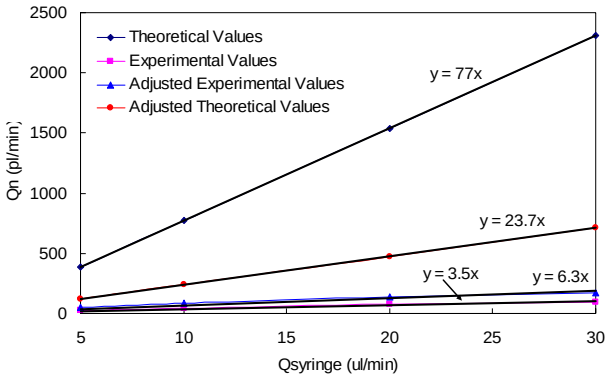

Figure 5. Nano-channel flow rates as a function of syringe, or equivalently, flow-driving micro-channel rates. Shown are the experimental values obtained by tracking flow in the serpentine micro-channel, the theoretical values calculated from Q_n/Q_m and the syringe flow rates, and the same curves adjusted for fabrication-caused dimension changes.

5 SUMMARY

Our novel active nanofluidic flow control configuration allows the primary problems of nanofluidic systems including interfacing and measuring to be successfully solved. We show that such a parallel approach makes it possible to have a broad range of fine flow rate control through the nanofluidic channel even with a system driven by a simple syringe pump. Flow rate differences between theoretical and experimental values were seen and these are shown to be due primarily to fabrication issues. Effects such as electrostatic interactions with the channel walls, wetting, and evaporation effects were shown to be secondary, at least for the DI water solution used.

ACKNOWLEGEMENTS

We thank Nadine B. Smith for allowing us to use the K&S 983 dicing saw in preparing our devices. We also acknowledge use of facilities at the PSU site of NSF NNIN. The project was supported in part by NSF Grant No. DMI-0615579.

REFERENCES

[1] G. Hu and D. Li, Chemical Engineering Science. 62, 3343, 2007.
[2] R. Karnik, K. Castelino, C. Duan and A. Majumdar, Nano Letter. 6, 1735, 2006.
[3] A. Malave, M. Tewes, T. Gronewold and M. Lohndorf, Microelectronic Engineering. 78, 587, 2005.
[4] F. H. J. Van Der Heyden, D. Stein and C. Dekker, Physical Review Letters. 95, 116104, 2005.
[5] E. Tamaki, A. Hibara, H. B. Kim, M. Tokeshi and T. Kitamori, J. Chromatogr. A. 1137, 256, 2006.
[6] J. P. Brody, P. Yager, R. E. Goldstein and R. H. Austin, Biophysical Journal. 71, 3430, 1996.
[7] P. Nath, S. Roy, t. Conlisk, and A. J. Fleischman, Biomedical microdevices. 7, 169, 2005.
[8] K. J. A. Westin, C. H. Choi and K. S. Breuer, Experiments in Fluids. 34, 635, 2003.